# Scope and computational insights into enantioselective C–H amination through silver-catalyzed nitrene transfer

Emily Z. Schroeder,[1‡] Yue Fu,[2‡] Jed Kim,[1] Wentan Liu,[1] Peng Liu,[2,*] Jennifer M. Schomaker[1,*]

[1] *Department of Chemistry, University of Wisconsin-Madison, 1101 University Avenue, Madison, WI 53706, USA*
[2] *Department of Chemistry, University of Pittsburgh, 219 Parkman Ave, Pittsburgh, PA 15260, USA*

KEYWORDS silver, nitrene transfer, asymmetric, amination, C-H functionalization

**ABSTRACT:** Chiral, non-racemic amines and amino alcohols are prevalent in drugs, bioactive natural products and ligands for transition metal catalysis. Asymmetric nitrene transfer is an efficient and powerful strategy to prepare enantioenriched amines from abundant C–H bonds; however, there is a continued need for general and inexpensive transition metal catalysts supported by easily tunable ligands. Herein, we report silver salts ligated to an unusual bis(oxazoline) (BOX) ligand, readily accessible through a modular synthetic approach, catalyze site- and enantioselective nitrene transfers into benzylic, allylic and unactivated C–H bonds of carbamate esters. The resulting 1,3-aminoalcohol building blocks are delivered in good yields and moderate-to-excellent enantioselectivities up to 99%. Computational models were employed to rationalize the observed stereochemical outcomes and set the stage for the predictive design of second-generation silver catalysts. These in-depth computational investigations implicate a complex combination of features in promoting enantioselectivity, including substrate distortion from a square-planar geometry at silver and stabilizing C–H/π interactions between ligand and substrate. Careful analyses of the enantiodetermining transition states employing diverse substrates revealed the dominant factors controlling selectivity for each substrate class, thus enabling the rational design of ligand and catalyst combinations that furnish a broader scope of chemo-, site- and enantioselective C–H bond aminations.

## Introduction

Enantioselective transformations of targeted C–H bonds into new C–N bonds is a powerful method for the synthesis of valuable amine building blocks that occur frequently in nitrogen-containing natural products and pharmaceuticals.[1,2] Transition metal-catalyzed nitrene transfer (NT) is a popular strategy to streamline access to these important compounds by facilitating direct C–H to C–N bond amination. However, achieving predictable control over the chemo-, site- and enantioselectivity of an NT event can be challenging. This is particularly true for the preparation of diverse aminoalcohol building blocks that employ inexpensive transition metals supported by modular ligands.[3]

Enantioselective aminations of benzylic, allylic and unactivated C–H bonds with a variety of nitrene precursors have been reported to form nitrogen-containing heterocycles and acyclic derivatives that include γ-lactams,[4,5] sulfamides,[6-9] sulfamates,[11,12] diamines,[6,13] and amino alcohols.[11,12,14,15] γ-Aminoarylpropanols and β-aminoarylethanols, which are accessible *via* ring-opening of cyclic sulfamates or carbamates following the NT event, are particularly attractive targets, as they are found in diverse bioactive molecules, including dapoxetine,[16] the anti-cancer candidate capivasertib,[17] and CB1 inverse agonists for the potential treatment of obesity (Figure 1), among others.[18] In addition, the alcohol handle can be easily elaborated to furnish other useful enantioenriched amine scaffolds. Despite the utility of enantioenriched 1,2- and 1,3-aminoalcohols, asymmetric NT methods for their formation that display broad scope are scarce.

Previous reports of asymmetric C–H bond amination utilize sulfamates and pre-oxidized carbamates as nitrene pre-

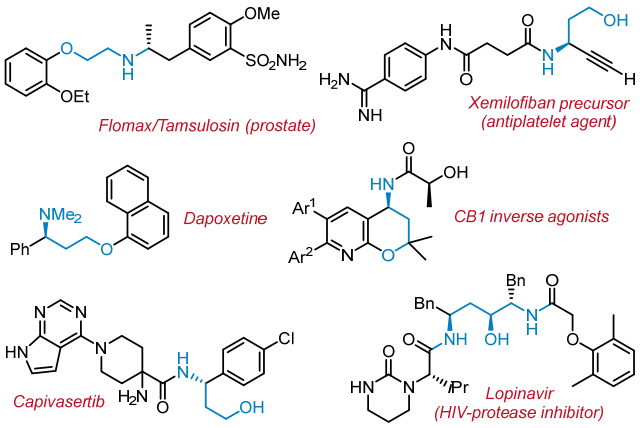


**Figure 1.** Aminoalcohol-containing bioactive molecules.

cursors (Scheme 1A) and precious metal catalysts. Du Bois found that the electronics of the aryl group impacted the *ee* of asymmetric benzylic C–H aminations catalyzed by dinuclear Rh complexes; the alkene geometry also played a role in the *ee* of the allylic amination. Blakey's Ru(pyBOX) catalyst was less sensitive to arene electronics in terms of *ee*, but

in contrast to $Rh_2$(*S*-NAP)$_4$, the (*Z*)-alkene gave lower *ee* than the *E* isomer. Davies and Meggers employed pre-oxidized carbamate-derived nitrene precursors with asymmetric Rh and Ru catalysts, but these were also limited in scope.[11,12,15] While progress continues to be made in predicting the origins of substrate effects on *ee*, in general, they are still not well understood prior to obtaining experimental results. Thus it is challenging to rationally design catalysts with high enantioselectivities for different substrate classes without extensive experimental screening and post-analysis.

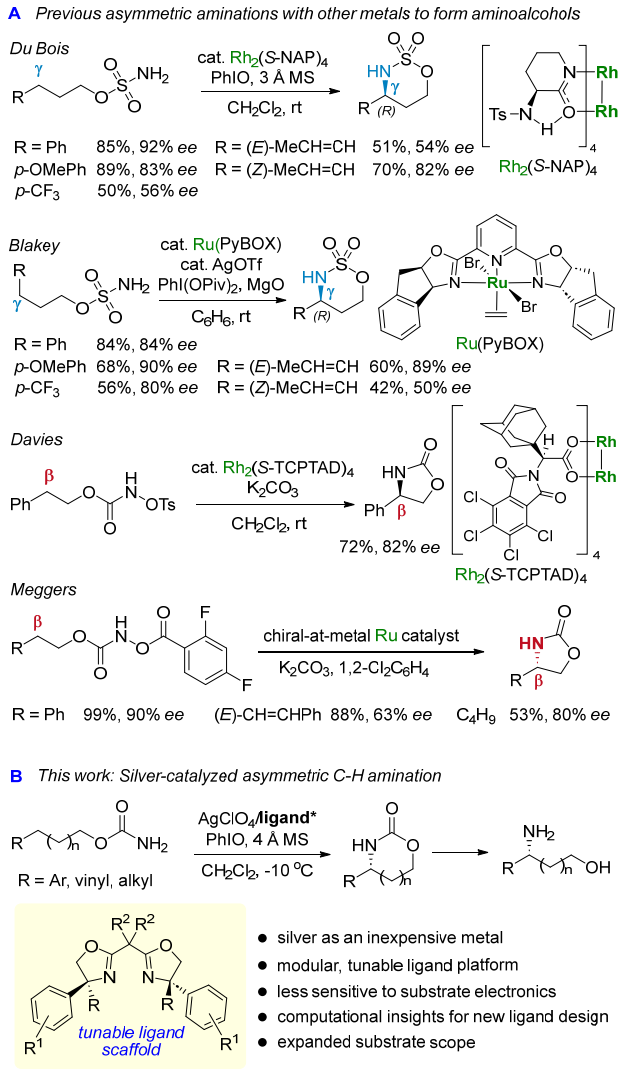


**Scheme 1.** Prior and proposed asymmetric C–H amination via NT to furnish amino alcohols.

We recently developed a new bis(oxazoline) ligand ((*S,S*)-Min-BOX, Scheme 1B, R = Me, R$^1$ = 3,5-di-*t*-Bu, R$^2$ = Me) for silver-catalyzed propargylic C–H bond amination in high *ee*.[19] Key features of the ligand include a fully substituted stereocenter on the oxazoline ring and significant steric bulk in the form of 3,5-$^t$Bu groups on the aryl ring. Initial attempts to expand the scope to encompass asymmetric aminations of benzylic, allylic and unactivated methylene C–H bonds were not promising and the limited modularity of our initial ligand synthesis further hampered efforts to identify key interactions between substrate and catalyst that could be tuned to improve scope. In light of these challenges, and to gain a thorough understanding of the factors responsible for high chemo-, site- and enantioselectivity within different substrate classes, we turned to computations to inform choices of substrate and catalyst that would furnish high *ee*. Herein, we report combined experimental and computational explorations of $AgClO_4$/(*S,S*)-Min-BOX and related catalysts that provide key insights into the mechanism and stereochemical models to enable future predictive catalyst designs for silver-catalyzed asymmetric intramolecular NT.

## Results and discussion

*Modular route to new bis(oxazoline) (BOX) ligands for asymmetric nitrene transfer.* Before embarking on computational studies to determine how changing the features of (*S,S*)-Min-BOX impact *ee*, a better and more modular route to Min-BOX and its analogues was required, as our first-generation synthesis suffered from several drawbacks.[19] Firstly, the route required an asymmetric Rh-catalyzed hydroformylation that employs a complex and commercially unavailable ligand, bis[(*S,S,S*)-DiazaPhos-SPE].[20] Only one enantiomer of this ligand can be easily prepared; thus only the (*S,S*)-Min-BOX enantiomer was accessible using our previous route. Secondly, utilizing a hydroformylation reaction as a key step in the synthesis limits us to the installation of a Me group at the fully substituted sp$^3$ carbon of the bis(oxazoline).[20]

To address these issues and provide a reliable and modular approach to analogues of both (*S,S*)-Min-BOX and (*R,R*)-Min-BOX, a new route to this class of ligands was developed (Scheme 2A). An asymmetric Rh-catalyzed boronic ester addition to imine **a** gave **b**,[21] which was further elaborated to (*S,S*)-Min-BOX using standard procedures. Employing the enantiomer of the *tert*-butylsulfinamide ligand gave facile access to (*R,R*)-Min-BOX, which was not available through our previous route.[19] In addition, this new strategy enables

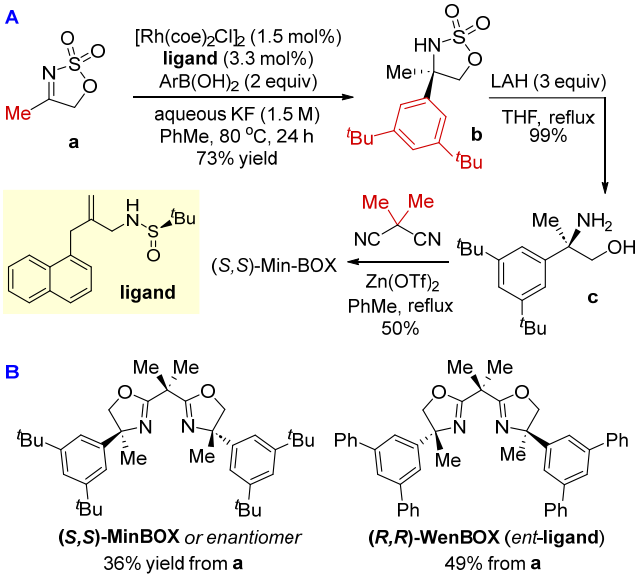


**Scheme 2.** New modular synthetic route to (*S,S*)- and (*R,R*)-Min-BOX and (*R,R*)-Wen-BOX.

easy manipulation of three diverse sites in the ligand, as highlighted in red. Using this approach, (*R,R*)-Wen-BOX was prepared (using the enantiomer of the sulfoxide ligand in Scheme 2A) to assess the differences in ligand performance when the bulky *tert*-butyl groups in (*S,S*)-Min-BOX are replaced with aryl groups that can potentially engage in π-π or other non-covalent interactions (NCIs) with the substrate (Scheme 2B).

*Benchmarking (S,S)-Min-BOX and (R,R)-Wen-BOX for the asymmetric amination of non-propargylic C–H bonds.* Studies to explore site- and enantioselective nitrene transfer (NT) with (*S,S*)-Min-BOX and (*R,R*)-Wen-BOX were initiated using three simple carbamates **1a-c**, bearing a benzylic, allylic and unactivated C–H bond, respectively (Table 1).[19] Treatment of **1a** with PhIO, 5 mol % $AgClO_4$ and 2.5 mol % (*S,S*)-Min-BOX at -10 °C for 48 h resulted in a moderate 54% yield of **2a** in promising 95:5 *er* (Table 1, entry 1). The site-selectivity was excellent, as no 5-membered ring product was observed. The role of the excess $AgClO_4$ is to serve as a Lewis acid to break down the polymeric PhIO and increase the overall rate and conversion of the reaction. Control experiments show minimal background reaction promoted by unligated $AgClO_4$. Reducing temperature in the reaction of **1a** to **2a** to -20 °C (entry 2) required increased catalyst loading and time; both the conversion and yield were improved, although the *er* was similar, suggesting no benefit to temperatures lower than -10 °C. Carrying out the reaction at room temperature reduced the *er* to 91:9 (entry 3), but gave complete conversion to **2a** in 99% yield. In cases where the product *er* can be easily increased through a simple recrystallization, this minimal reduction in *er* may be readily compensated for by the higher conversions and yields observed at rt. Ultimately, increasing the catalyst loading to 10 mol % $AgClO_4$ and 5 mol % (*S,S*)-Min-BOX and running the reaction at -10 °C gave a good balance between conversion and *er* (entry 4); these conditions were adopted for studies of the substrate scope. The (*R,R*)-Wen-BOX ligand at rt gave 58% yield of **2a** with 93:7 *er* of the opposite enantiomer (entry 5) and 34% remaining starting material. Increasing the ligand loading to 10 mol % (entry 6) at rt increased the yield to 86% at 92:8 *er*.

Substrate **1b**, bearing a sterically unhindered allylic C–H bond, showed similar yield and *ee* when switching from (*S,S*)-Min-BOX (entry 7, 79% yield, 77:23 *er*) to (*R,R*)-Wen-BOX (entry 8, 80%, 79:21 *er*). Site-selectivity was excellent, with no formation of the 5-membered ring. Interestingly, substrate **1c**, which displays an unactivated C($sp^3$)–H bond (entries 9, 10), gave a higher *er* of **2c** using (*R,R*)-Wen-BOX at rt. However, 24% of the five-membered ring was also noted (entry 10), suggesting that the Wen-BOX ligand may be more sensitive to steric effects with regards to the site-selectivity of the nitrene transfer event. This observation is explored further in Table 4 (*vide infra*).

Given the initial results in Table 1, we opted to first explore the scope of the most promising system involving the asymmetric amination of benzylic C–H bonds using (*S,S*)-Min-BOX as the ligand. We reasoned that the results would provide more insight into potential catalyst/substrate interactions with the capacity to impact the enantiomeric ratio. This key information could inform subsequent computational studies, with the ultimate goal of developing a

**Table 1.** Initial exploration of asymmetric amination of benzylic, allylic and unactivated C($sp^3$)–H bonds.

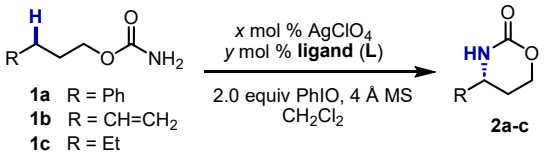


| entry | | mol% Ag | L, mol% | T (°C) | t (h) | yield **2** (*er*) |
|---|---|---|---|---|---|---|
| 1 | **1a** | 5 | (*S,S*)-Min-BOX, 2.5 | -10 | 48 | 60% **2a** (95:5) |
| 2 | **1a** | 20 | (*S,S*)-Min-BOX, 10 | -20 | 72 | 75% **2a** (96:4) |
| 3 | **1a** | 20 | (*S,S*)-Min-BOX, 10 | rt | 12 | 99% **2a** (91:9) |
| 4 | **1a** | 10 | (*S,S*)-Min-BOX, 5 | -10 | 48 | 90%[a] **2a** (95:5) |
| 5 | **1a** | 10 | (*R,R*)-Wen-BOX,[b] 5 | rt | 21 | 58%[a] **2a** (93:7) |
| 6 | **1a** | 20 | (*R,R*)-Wen-BOX,[b] 10 | rt | 20 | 86%[a] **2a** (92:8) |
| 7 | **1b** | 10 | (*S,S*)-Min-BOX, 5 | -10 | 48 | 79%[a] **2b** (77:23)[c] |
| 8 | **1b** | 10 | (*R,R*)-Wen-BOX,[b] 5 | -10 | 48 | 80%[a] **2c** (79:21)[c] |
| 9 | **1c** | 10 | (*S,S*)-Min-BOX, 5 | -10 | 24 | 26%[a] **2c** (69:31)[c,d] |
| 10 | **1c** | 10 | (*R,R*)-Wen-BOX,[b] 5 | rt | 21 | 38%[a] **2c** (75:25)[c,e] |

Yields determined by $^1$H NMR with mesitylene and trimethylphenylsilane internal standards. [a] Isolated yields. [b] Enantiomer of the product obtained with (*S,S*)-Min-BOX. [c] *er* was determined after benzylation. [d] 5% of the 5-membered ring. [e] 24% of the 5-membered ring in 56:44 *er*.

feasible stereochemical model that is capable of informing both substrate and catalyst designs to achieve high *ee* in the aminations of diverse C–H bonds, including challenging allylic and unactivated C–H bonds.

*Scope of asymmetric benzylic C–H bond amination.* With optimized conditions in hand, the scope of the enantioselective C–H amination was explored (Table 2) and the performance of (*S,S*)-Min-BOXAgClO$_4$ assessed compared to Rh and Ru catalysts (Scheme 1A). In general, the high *ee* of the reaction was maintained across a variety of carbamates containing benzylic C–H bonds. Changing the electronics of the arene though the addition of electron-withdrawing or electron-donating groups in the *para*-position (**2a**, **3a-7a**) did not significantly impact *er*. Precursor **6**, bearing a *p*-OMe group gave **4a** in 95:5 *er*, while **7**, bearing a *p*-$CF_3$ group, gave **7a** in a similar *er* of 94:6. Interestingly, this is in contrast to results observed with both the Du Bois $Rh_2$(*S*-NAP)$_4$ and the Blakey Ru(pyBOX) catalysts,[11,12] although steric effects cannot be completely ruled out in these examples. As expected, more electron-poor C–H bonds typically underwent amination at slower rates under the standard conditions, resulting in only ~50% conversion for substrates **4a**-**6a**. However, increasing the amount of the silver salt to 20 mol % improved the conversion of the nitrene transfer with little impact on the *er*. Substitution at the α-position of the carbamate tether in **8** enhanced the reactivity to furnish **8a** in excellent yield and *er*, even at reduced catalyst loadings. Interestingly, ad-

**Table 2.** Scope for asymmetric silver-catalyzed amination of benzylic C–H bonds.

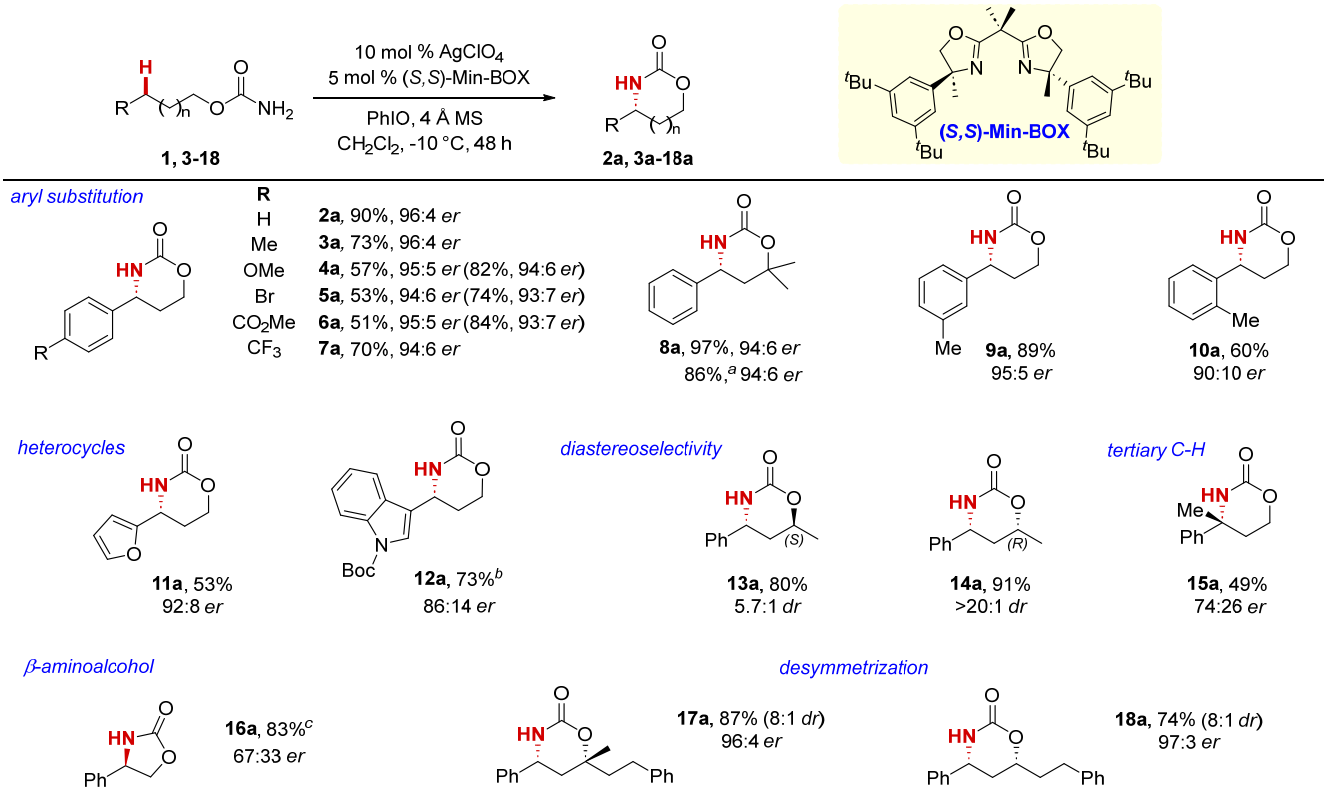


Yields and *er* values in parenthesis were run with 20 mol % $AgClO_4$. [a] 5 mol % $AgClO_4$, 2.5 mol % (*S,S*)-Min-BOX. [b] 20 mol % $AgClO_4$, 10 mol % (*S,S*)-Min-BOX, room temp. [c] 18-20 h at room temperature.

dition of a Me group at the *meta* position of **9** resulted in a maintained *er* of **9a** at 95:5, while moving the Me group to the *ortho* position in **10** resulted in an *er* of 90:10 for **10a**. Electron-rich heterocycles were also tested in the asymmetric nitrene transfer; furan **11a** was obtained in good *er*, with the lower yield attributed to competing oxidative degradation of the sterically accessible furan ring. Finally, the indole derivative **12** was poorly reactive at -10 °C, but gave moderate yield and *er* of **12a** at room temperature.

Substrates containing a stereogenic carbon were also investigated to probe how the nature of the catalyst impacts the diastereoselectivity of the silver-catalyzed amination. Carbamates **13** and **14** were prepared in enantioenriched form from the corresponding secondary alcohols and individually subjected to the reaction conditions. Utilizing (*S,S*)-Min-BOX with the (*R*) enantiomer **14** increased the *dr* for the *syn* diastereomer **14a** to >20:1, compared to the 3.4:1 *syn:anti* ratio observed when the same reaction was run with an achiral bis(oxazoline) ligand (see SI for details). Subjecting the (*S*) enantiomer **13** to standard reaction conditions resulted in the catalyst selecting for the typically disfavored *anti*-diastereomer **13a** in a 5.7:1 *dr*. This is particularly noteworthy, as enantioenriched *trans*-1,3-aminoalcohols are not accessible using other reported catalyst systems, which overwhelmingly favor the *syn* diastereomer.[3]

To further challenge our asymmetric amination chemistry, a carbamate **15** bearing a tertiary benzylic C–H bond was investigated. With a typical racemic catalyst, NT likely occurs via a concerted C–H amination or by H-atom abstraction, followed by rapid radical rebound. However, we were curious whether a mismatch between (*S,S*)-Min-BOX and the stereochemistry at a racemic tertiary C–H bond could lead to a longer-lived radical intermediate, where the initial stereochemistry could be ablated and reset by the catalyst. Running the amination of **15** under the standard reaction conditions resulted in 49% yield of the product **15a** and 49% recovery of the starting material **15**. However, the *er* of both compounds were 74:26. This suggests a scenario involving moderate kinetic resolution by (*S,S*)-Min-BOX, influenced by the small difference between the two activation barriers for C–H amination of (*R*)-**15** vs. (*S*)-**15**. However, (*S,S*)-Min-BOX$AgClO_4$ did prove capable of desymmetrizing benzylic C–H bonds in good *er*. Subjecting the achiral carbamates **17** and **18** to the standard reaction conditions resulted in an effective desymmetrization of both compounds to provide the corresponding benzylic amines **17a** and **18a** in excellent yield, *dr* and *er*.

We were also curious if the (*S,S*)-Min-BOX ligand would be capable of furnishing good *ee* in the silver-catalyzed amination of homobenzylic carbamates that bear one less carbon in the tether to deliver enantioenriched 1,2-aminoalcohols. Reaction of **16** at room temperature gave a good yield of **16a**, albeit in a low 67:33 *er*. Additionally, the *er* was not improved by lowering the temperature. Nonetheless, this result, when combined with results showing the impact of the sterics of arene substitution on the *er* (Table 2, **9a-10a**), provided valuable information to inspire our computational investigations on factors affecting catalyst–substrate interactions and the effectiveness of enantioinduction in the selectivity-determining transition states (*vide infra*).

*Computational explorations of asymmetric silver-catalyzed C–H bond amination with (S,S)-Min-BOX*. Density functional theory (DFT) calculations[22] were performed to investigate the origin of enantioselectivity in the Ag-catalyzed benzylic C–H amination and to better understand why the Min-BOX ligand leads to high *ee* with benzylic and heterobenzylic precursors, but is less effective with substrates containing sterically unhindered allylic (Table 1, **1b**) or unactivated methylene C–H bonds (**1c**). DFT and local coupled cluster theory [PNO-LCCSD(T)-F12][23] calculations indicated that the singlet Ag nitrene C–H insertion pathway is more favorable than the competing triplet pathway (see Figure S1 in the SI for details).[24] This singlet pathway involves concerted C–H bond cleavage and C–N bond formation without the formation of an alkyl radical intermediate; therefore, the enantioselectivity is determined in this concerted C–H insertion transition state (TS). The most stable C–H insertion TS isomers with the benzylic substrate **1a** (Figure 2) involve a four-coordinate square-planar Ag nitrene complex, where the carbamate carbonyl coordinates to the Lewis acidic Ag center. Several alternative TS isomers were also considered, including a trigonal planar Ag nitrene lacking the carbamate carbonyl–Ag coordination, a TS with a partially dissociated monodentate Min-BOX ligand having only one oxazoline nitrogen bound to the Ag, and finally, a TS having an *N,O*-bidentate binding mode for (*S,S*)-Min-BOX (Figures S2 and S3). All of these alternative TS isomers are higher in energy than those involving the four-coordinate square-planar Ag nitrene complex where the carbamate carbonyl group is coordinated to Ag. This C–H insertion mechanism involving a singlet square-planar Ag nitrene is consistent with our recent computational study of nitrene transfer using an achiral 2,2'-isopropylidenebis(4,4'-dimethyl-2-oxazoline)-supported (dmBOX) Ag catalyst.

*Asymmetric amination of benzylic C–H bonds.* Next, we analyzed the origins of enantioselectivity in the benzylic amination of **1a**. Two ring-flipped conformers of the seven-membered cyclic C–H insertion TS were located for the activation of each prochiral benzylic C–H bond (Figure 2). The computed enantioselectivity is consistent with the experimental results, where the most favorable C–H insertion transition state **TS1** ($\Delta G^{\ddagger}$ = 6.6 kcal/mol with respect to the Ag nitrene intermediate) leads to the observed major enantiomeric product, (*R*)-**2a**. The two transition state conformers (**TS2** and **TS4**) that lead to the *S* enantiomer of the product (*S*)-**2a** are both 3.9 kcal/mol higher in energy than **TS1**. The enantioselectivity is attributed to steric repulsions between the Ph substituent on the benzylic substrate and the C2-symmetric (*S,S*)-Min-BOX ligand that led to greater distortion of the disfavored transition states. In all four C–H insertion transition states (**TS1**–**TS4**), the nitrene moiety in the four-coordinate Ag complex is slightly distorted from the preferred square planar geometry due to steric repulsions with the Ar group on the (*S,S*)-Min-BOX ligand located in quadrant **IV**. This sterically induced distortion is more profound in **TS2** and **TS4**, where the Ph group of the substrate would be placed in a quadrant (**IV**) occupied by the bulky Ar group if the nitrene was not distorted. In the optimized structures of **TS2** and **TS4**, the Ph group is placed in the less occupied quadrant **I**, resulting in a more distorted square-planar geometry. Such distortion weakens the Ag–carbamate carbonyl coordination and leads to longer Ag···O(carbonyl) distances in **TS2** and **TS4** (2.22 and 2.20 Å, respectively) than those in **TS1** and **TS3** (both are 2.18 Å). In **TS1** and **TS3**, the Ph group is placed in the unoccupied quadrant **I**, and thus such ligand–substrate steric repulsions are diminished. In addition, **TS1** is stabilized by a C–H/π interaction between the Ph group on the substrate and the *t*-Bu group on the ligand. The ring-flipped TS conformer **TS3** is 2.2 kcal/mol less stable than **TS1** because the Ph group is in a pseudoaxial position, rather than the pseudoequatorial position as in **TS1**.

Next, we investigated substrate effects on enantioselectivity by comparing the C–H insertion TS with the sterically un-

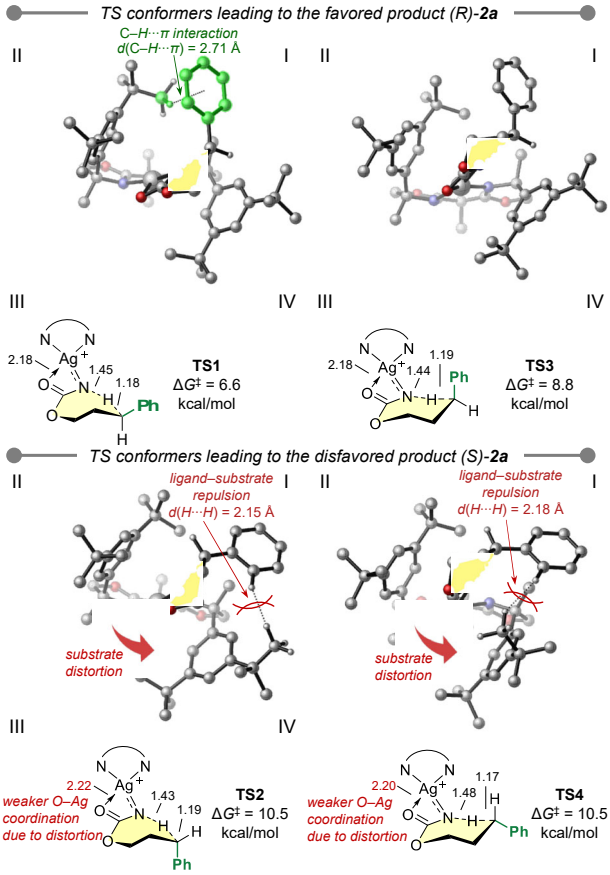


**Figure 2**. C–H insertion transition state structures of the asymmetric NT of benzylic substrate **1a**. Gibbs free energies of activation are with respect to the Ag nitrene intermediate. (*S,S*)-Min-BOX ligand was used in the calculations.

hindered allylic substrate (**1b**) and a benzylic substrate with a shorter tether (**16**) (Figure 3). The computed enantioselectivities for **1b** and **16** are both lower than that of **1a** ($\Delta\Delta G^{\ddagger}$ = 0.7 and 2.5 kcal/mol for **1b** and **16**, respectively, compared to $\Delta\Delta G^{\ddagger}$ of 3.9 kcal/mol for **1a**), which is consistent with the lower *er* observed experimentally. In the allylic C–H insertion transition state (**TS6**) leading to the minor product (*S*)-**2b**, the smaller alkenyl group in **1b** compared to the Ph group in **1a** diminishes the steric repulsion with the (*S,S*)-Min-BOX ligand. This means that the alkenyl group can be placed in the occupied quadrant **IV** without distorting the square planar geometry of the Ag nitrene. Moreover, in **TS5** leading to the major product (*R*)-**2b**, the

stabilizing non-covalent interactions between the ligand and the smaller alkenyl group are weaker than the C–H/π interaction observed in **TS1** with the benzylic substrate **1a**. Therefore, both factors lead to diminished enantioselectivity with the allylic substrate. Similarly, in the C–H insertion with **16**, the ligand–substrate steric repulsion in **TS8** leading to the minor product (*S*)-**16a** is also diminished, because the six-membered cyclic TS is sterically less encumbered than the seven-membered TS with **1a**. The greater ligand–substrate distance allows the Ph group on the substrate to be placed in the occupied quadrant (**IV**) without distorting the Ag nitrene in order to maintain the preferred square planar geometry. **TS7** that leads to the major enantiomeric product contains a ligand–substrate C–H/π interaction similar to **TS1**; however, due to the smaller ring size, a greater substrate distortion is required to orient the Ph group towards the Ar group in quadrant **II**. This distortion leads to a longer Ag···O(carbonyl) distance of 2.22 Å in **TS7**, compared to 2.20 Å in **TS8**. Taken together, the computed C–H insertion transition states with substrates **1a**, **1b**, and **16** revealed two concurrent factors affecting enantioselectivity: ligand–substrate steric repulsions that destabilize the TS leading to the minor enantiomeric product, and C–H/π interactions between the *t*-Bu group on the Min-BOX ligand and the Ph group on the benzylic substrate in the TS leading to the major enantiomeric product. The lower *er* observed with less sterically demanding substrates (*e.g.*, **1b**) and substrates with a shorter tether (*e.g.*, **16**) is because one or both of these interactions are diminished.

We surmised that the enantioselectivities of challenging substrates, such as **1b**, might be enhanced by rationally tuning the substituents on the Min-BOX ligand or substrate steric properties to enhance the stabilizing non-covalent interactions in the favored TS, as well as the steric repulsions and substrate distortions in the disfavored TS. Because the computed TS structures indicated insufficient catalyst–substrate interactions due to the smaller size of the allyl moiety in **1b** (Figure 3), we surmised that the desired interactions could be enhanced by using a more hindered (*S,S*)-Wen-BOX ligand, where the 3,5-di-*tert*-Bu phenyl substituents in (*S,S*)-Min-BOX were replaced with 3,5-di-Ar phenyl groups.

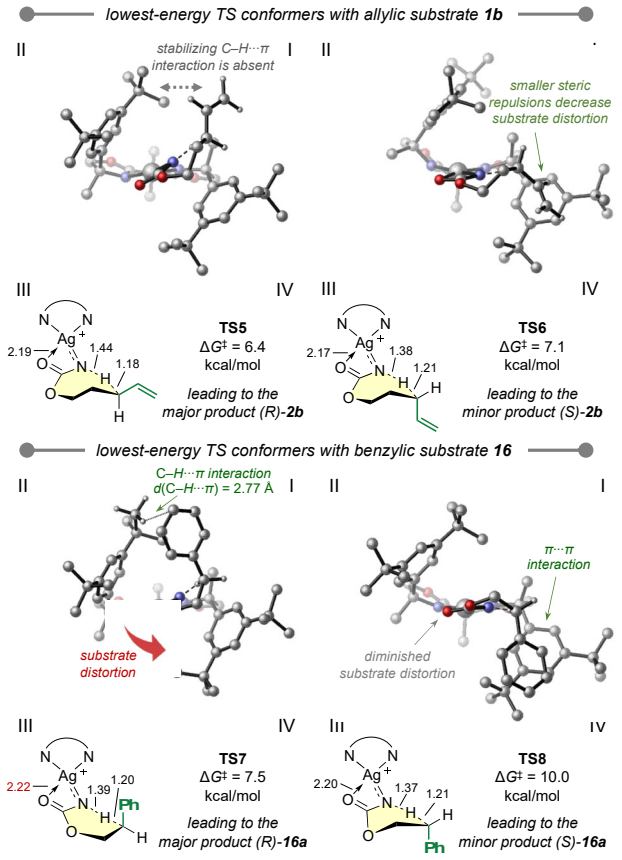


**Figure 3**. Origins of diminished enantioselectivity in the C–H amination of allylic substrate **1b** and benzylic substrate **16** with a shorter tether. Gibbs free energies of activation are in kcal/mol with respect to the singlet Ag nitrene intermediate. (*S,S*)-Min-BOX ligand was used in the calculations.

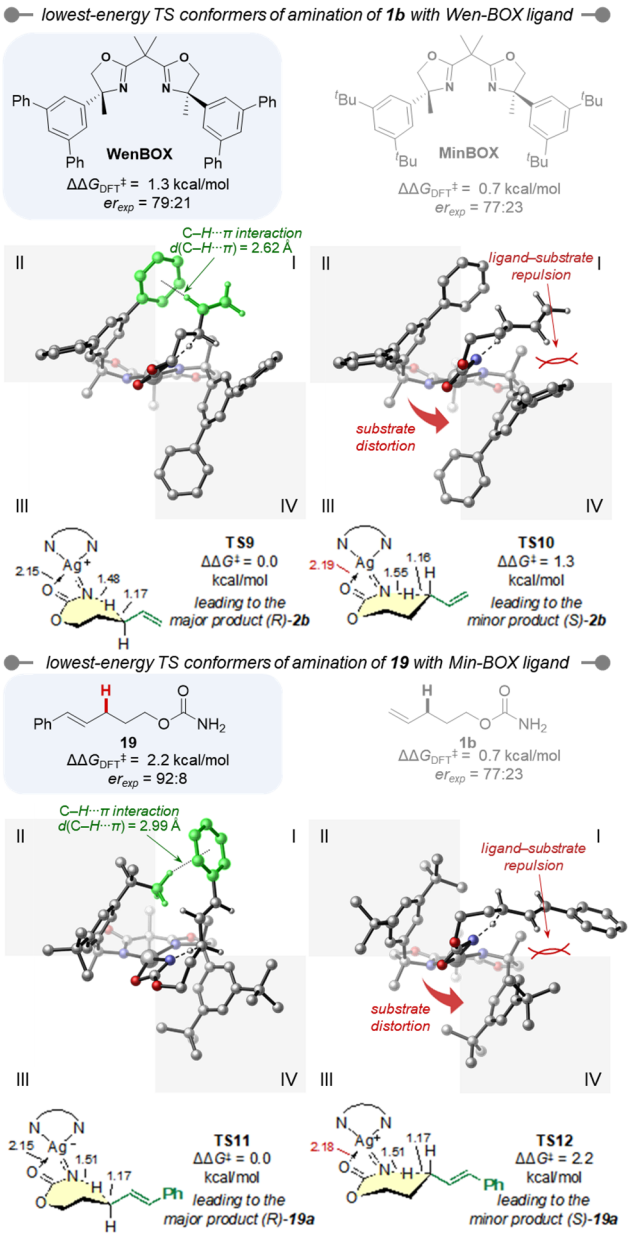


**Figure 4**. Ligand and substrate effects on the enantioselectivity.

Indeed, the computations indicated a small increase of enantioselectivity in the C–H amination of **1b** (Figure 4, $\Delta\Delta G^{\ddagger}$ = 1.3 kcal/mol compared to 0.7 kcal/mol in the reaction with Min-BOX). Here, the transition state (**TS9**) leading to the major product is stabilized by C–H/π interactions between the alkenyl C–H on the substrate and the newly introduced Ph group on the ligand. In addition, the transition state leading to the minor product, **TS10**, suffers from greater ligand–substrate steric repulsions in the occupied quadrant **IV** that distort the Ag nitrene to the non-square-planar conformation with a longer Ag···O(carbonyl) distance (2.19 Å, vs 2.15 Å in **TS9**). Although the *er* improvement is small (Table 1, entry 8), in part due to the relatively small energy penalty for substrate distortion to avoid unfavorable steric repulsions in the disfavored C–H insertion TS, this example highlights the feasibility of using computed TS structures to rationally design more selective amination catalysts by fine-tuning catalyst–substrate non-covalent interactions.

As our computational models (Figures 2-4) indicated that the substrate identity is expected to exert a large effect on the distortion or stabilization of the relevant flexible 7-membered transition states, the enhancement of catalyst-substrate interactions was investigated through the use of more sterically demanding alkenes. Gratifyingly, the computed transition states of styrenyl substrate **19** with (*S,S*)-Min-BOX ligand led to increased *er* (92:8, Table 3) compared to the allylic substrate **1b** with the same ligand ($\Delta\Delta G^{\ddagger}$ = 2.2 and 0.7 kcal/mol for **19** and **1b**, respectively). The newly introduced Ph group on **19** enables stabilizing C–H/π interactions with the *tert*-Bu group on the (*S,S*)-Min-BOX ligand (quadrant **II**) in **TS11** leading to the major enantiomeric product. In addition, replacing the vinyl group with the larger styrenyl moiety increases ligand–substrate steric repulsion in the **TS12** that gives the minor enantiomeric product, leading to the same substrate distortion observed

**Table 3.** Scope of asymmetric silver-catalyzed amination of allylic C–H bonds.

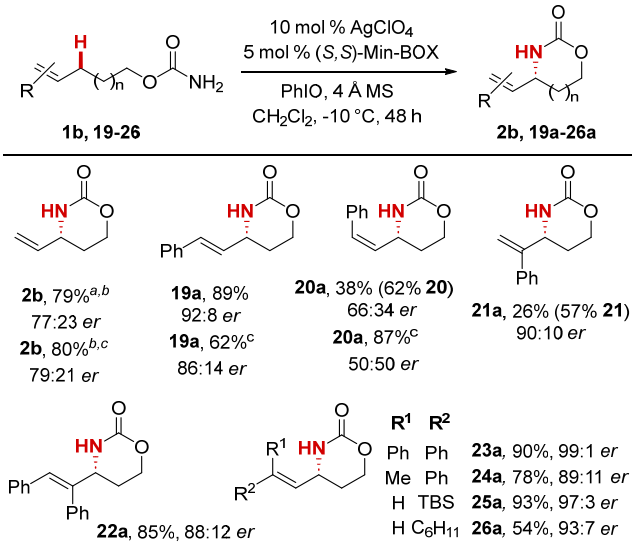


[a] Reaction was run for 24 h. [b] *er* was determined after benzylation. [c] 5 mol % (*R,R*)-WenBOX was employed at rt for 48 h to give the enantiomer of **2b**.

in other disfavored TS isomers, including **TS2** and **TS10**. Therefore, the higher *er* with **19** indicates that the alkenyl substituent on the substrate also affects non-covalent ligand–substrate interactions and substrate distortion, and ultimately, the *er* of the amination product. This prompted us to experimentally explore the scope of diverse allylic substitution patterns to further understand these effects on reactivity and *er*.

As already shown in Table 1, amination of **1b** gave higher *er* with (*R,R*)-Wen-BOX as compared to (*S,S*)-Min-BOX, even though the former reaction was run at higher temperature, which accounts for the increased conversion and yield with (*R,R*)-Wen-BOX. However, the trends in conversion and yield with substituted alkenes **19-26** using (*S,S*)-Min-BOX proved puzzling. Unsubstituted, *cis*- or 2,2'-disubstituted alkenes (**1b**, **20**, **21**) gave poor conversions to the desired **2b**, **20a** and **21a**, with *er* values varying from 66:34 to 90:10. Interestingly, the presence of a *trans*-substituent on the alkene, whether aryl (**19**, **22-24**) or alkyl/heteroalkyl (**25**, **26**), significantly improved the yield of the reaction and resulted in good-to-excellent *er*. For example, an aryl group could be accommodated at the internal alkene carbon of **22** to give **22a** in 85% yield and 88:12 *er*, while moving the phenyl to the terminal carbon of **23** improved the yield and *er* to 90% and >99:1, respectively. We hypothesize that the low conversion and *er* for **1b** and **20-21** may result from competing binding of the silver center to the alkene, as alkenes are well-known to serve as ligands for silver. Certain alkene substitution patterns may favor binding to the metal as a hemi-labile ligand that impedes reactivity and/or promotes background reaction.[25] Decreasing the size of the group *cis* to the group undergoing amination from Ph in **23** to a Me in **24** resulted in a decreased in *er* of **24a** to 89:11. A bulky TBS group in **25** gave **25a** in excellent *er*, suggesting that steric bulk in the *trans* position is important to achieve high *er*. Replacing the *trans* H group of **1b** with a cyclohexyl group in **26** improved the *er* of the allylic amine products from 73:27 in **2b** to 93:7 in **26a.** Unfortunately, attempts to utilize (*R,R*)-Wen-BOX to improve the *er* of substituted alkenes **19** and **20** reduced the *er* for both substrates, highlighting the impact of small changes in the ligand that lead to larger and more varied energetic interactions in the enantiodetermining TS.

*Asymmetric amination of unactivated C–H bonds.* Chemocatalyzed asymmetric aminations of unactivated prochiral C–H bonds to form enantioenriched 1,3-aminoalcohols remain a challenge in the field of NT. We explored a series of alkyl-substituted carbamates (Table 4) using (*S,S*)-Min-BOX and (*R,R*)-Wen-BOX as ligands. A small alkyl group proximal to the γ site for C–H insertion, such as the ethyl chain in **1c**, gave a 69:31 *er* with (*S,S*)-Min-BOX, which improved to 75:25 *er* using the bulkier (*R,R*)-Wen-BOX. Increasing the length of the alkyl group in **27** improved the *er* of **27a** to 79:21 using (*S,S*)-Min-BOX, with a slight decrease to 76:24 *er* using (*R,R*)-Wen-BOX. The greater steric pressure exerted by the (*R,R*)-Wen-BOX ligand was supported by the observation that reaction of **27** resulted in reduced reactivity even at rt, and also furnished 15% of the five-membered ring byproduct. Similar results were obtained with **28**; in this case, the site-selectivity for 6- vs. 5-membered ring eroded to nearly 1:1 using (*R,R*)-Wen-BOX. Moving the

steric bulk closer to the γ C–H bond gave 83:17 *er* for **29a** in excellent yield, but too much additional bulk in **30a** again decreased the *er*. Carbamates **31** and **32** were tested to assess whether a pendant aryl group might engage in product-

**Table 4.** Scope of asymmetric silver-catalyzed amination of unactivated C(sp$^3$)–H bonds.

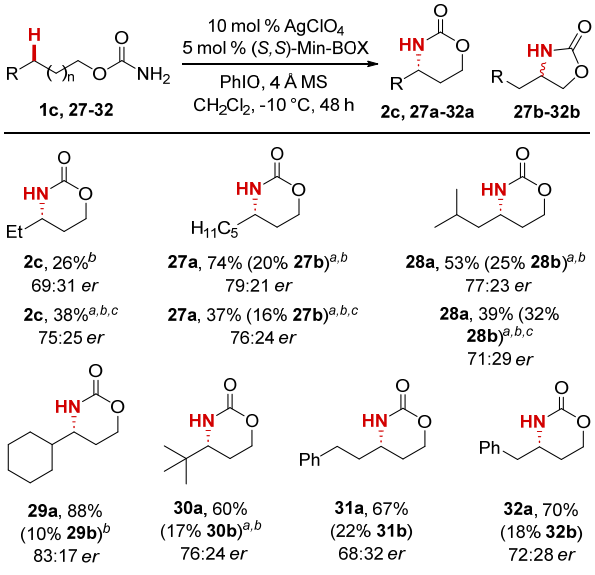


[a] 18-20 h at rt. [b] *ee* was determined after benzylation. [c] 5 mol % of (*R,R*)-Wen-BOX was used instead of (*S,S*)-Min-BOX.

ive non-covalent interactions with the ligand to improve the *ee*; however, **31a** and **32a** showed a surprising reduction in *er* to 68:32 and 72:28, respectively. These informative results highlight the challenges associated with the asymmetric amination of unactivated C–H bonds when both site- and enantioselectivity must be controlled. The response of substituents of varying steric bulk to changing the ligand from (*S,S*)-Min-BOX to (*R,R*)-Wen-BOX, combined with computational insights into the major interactions in the transition states that control for site- and enantioselectivity, provides valuable insight for the design of second-generation ligands moving forward.

The utility of the asymmetric nitrene transfer was demonstrated in a short synthesis of the drug Dapoxetine (Scheme 3). The ability to access (*R,R*)-Min-BOX (Scheme 1) enabled

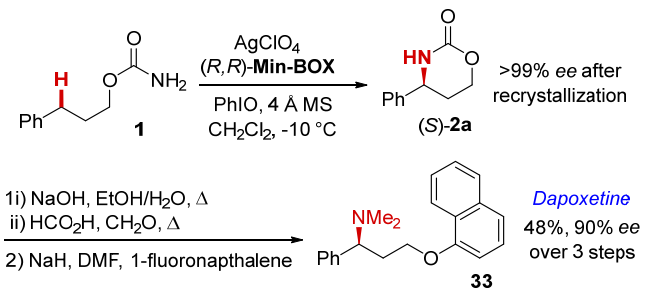


**Scheme 3.** Demonstration of asymmetric benzylic C–H amination via NT to a short synthesis of the drug Dapoxetine.

preparation of the desired (*S*)-enantiomer of **2a**. After recrystallization of (*S*)-**2a** to improve the *ee* to 99%, the carbamate ring was hydrolyzed with NaOH. The free amino alcohol product was carried forward without purification and subjected to Eschweiler-Clarke reaction conditions. Finally, Dapoxetine was synthesized in 48% overall yield and 90% *ee* via a $S_NAr$ reaction of the methylated amino alcohol with 1-fluoronaphthalene.

## Conclusion

In conclusion, we report an enantioselective silver-catalyzed amination of diverse C–H bonds that proceeds via a nitrene transfer pathway. The designer bis(oxazoline) ligands Min-BOX and Wen-BOX are key to furnishing good *ee* for benzylic amination of both electron-rich and electron-poor aromatic rings bearing a variety of functional groups. Other attractive features include high diastereo- and enantioselectivity in the desymmetrization of benzylic C–H bonds, the ability of (*S,S*)-Min-BOX to override inherent substrate control to access enantioenriched 1,3-*anti*-aminoalcohols. Computational studies showed that a combination of two key features promote high *er*, including substrate distortion from a square-planar geometry at silver and stabilizing C–H/π interactions between the chiral ligand and the substrate. Computed transition state structures with substrates that furnished lower *er* showed weaker dispersion interactions that diminished stabilizing effects in TS, as well as smaller steric-induced silver nitrene distortion that led to ineffective enantiodiscrimination. In addition, the effects of tether lengths on catalyst–substrate interactions and enantioselectivity were also analyzed computationally. These insights were employed to identify other substrates that ultimately gave high *er* for amination of allylic C–H bonds and moderate *er* for amination of unactivated alkyl C(sp$^3$) C–H bonds. Computations also shed insight into an improved ligand design (Wen-BOX), while highlighting the feasibility of using computed TS structures to rationally design more selective catalysts by fine-tuning catalyst–substrate steric and non-covalent interactions to improve enantioinduction with challenging substrates that lack sufficient enantioselectivity control with the previous generation catalyst, Min-BOX. Finally, the utility of silver-catalyzed asymmetric benzylic amination was demonstrated in a short synthesis of the drug Dapoxetine. Ultimately, the melding of experimental and detailed computational studies revealed the importance of subtle effects on *er* and sets the stage for the predictive design of second-generation silver catalysts.

## ASSOCIATED CONTENT

Characterization data, optimization tables, additional substrates/catalysts, and details of computational methods are included in the supplementary materials, which are available free of charge via the Internet at http://pubs.acs.org.

## AUTHOR INFORMATION

### Corresponding Authors

* schomakerj@chem.wisc.edu
* pengliu@pitt.edu

### Author Contributions

The manuscript was written through contributions of all authors. All authors have given approval to the final version of the manuscript.


## Funding Sources

J.M.S. is grateful to NSF 1954325 for financial support of this research. The Paul Bender Chemistry Instrumentation Center includes: Thermo Q ExactiveTM Plus by NIH 1S10 OD020022-1; Bruker Avance-500 by a generous gift from Paul J. and Margaret M. Bender; Bruker Avance-600 by NIH S10 OK012245; Bruker Avance-400 by NSF CHE-1048642. P.L. acknowledges the NSF (CHE-2247505) for financial support. DFT calculations were carried out at the University of Pittsburgh Center for Research Computing and the Advanced Cyberinfrastructure Coordination Ecosystem: Services & Support (ACCESS) program, supported by NSF award numbers OAC-2117681 and OAC-2138259.

## ACKNOWLEDGMENT

Dr. Charles G. Fry, Dr. Heike Hofstetter, and Dr. Cathy Clewett at UW-Madison are thanked for help with NMR techniques. Dr. Martha M. Vestling at UW-Madison is thanked for mass spectrometry characterization. UCSF Chimera is developed by the Resource for Biocomputing, Visualization, and Informatics at the University of California, San Francisco (supported by NIH P41-GM103311).


## REFERENCES


1. Heravi, M.; Zadsirjan V. Prescribed Drugs Containing Nitrogen Heterocycles: An Overview *RSC Adv.* **2020**, *10*, 44247–44311.
2. Ricci, A. *Amino Group Chemistry: From Synthesis to the Life Sciences*; Wiley: Weinheim, 2008.
3. For selected reviews see: (a) Collet, F.; Lescot, C.; Dauban, P. Catalytic C-H Amination: The Stereoselectivity Issue. *Chem. Soc. Rev.* **2011**, *40*, 1926–1936. (b) Uchida, T.; Hayashi, H. Recent Development in Asymmetric C-H Amination via Nitrene Transfer Reactions. *Eur. J. Org. Chem*. **2020**, 909-916. (c) Ju, M.; Schomaker, J. M. Nitrene Transfer Catalysts for Enantioselective C–N Bond Formation. *Nat. Rev. Chem.* **2021**, 5, 580-594.
4. Park, Y.; Chang, S. Asymmetric Formation of γ-Lactams via C–H Amination Enabled by Chiral Hydrogen-Bond-Donor Catalysts. *Nat. Catal*. **2019**, *2*, 3, 219–227.
5. Xing, Q.; Chan, C. M.; Yeung, Y. W.; Yu, W. Y. Ruthenium(II)-Catalyzed Enantioselective γ-Lactams Formation by Intramolecular C-H Amination of 1,4,2-Dioxazol-5-Ones. *J. Am. Chem. Soc.* **2019**, *141*, 9, 3849–3853.
6. Li, C.; Lang, K.; Lu, H.; Hu, Y.; Cui, X.; Wojtas, L.; Zhang, X. P. Catalytic Radical Process for Enantioselective Amination of C(Sp3)−H Bonds. *Angew. Chem. Int. Ed.* **2018**, *57*, 16837-16841.
7. Lang, K.; Torker, S.; Wojtas, L.; Zhang, X. P. Asymmetric Induction and Enantiodivergence in Catalytic Radical C-H Amination via Enantiodifferentiative H-Atom Abstraction and Stereoretentive Radical Substitution. *J. Am. Chem. Soc.* **2019**, *141*, 31, 12388–12396.
8. Lang, K.; Li, C.; Kim, I.; Zhang, X. P. Enantioconvergent Amination of Racemic Tertiary C–H Bonds. *J. Am. Chem. Soc.* **2020**, *142*, 20902–20911.
9. Yang, Y.; Cho, I.; Qi, X.; Liu, P.; Arnold, F. H. An Enzymatic Platform for the Asymmetric Amination of Primary, Secondary and Tertiary C($sp^3$)–H Bonds. *Nat. Chem.* **2019**, *11,* 987–993.
10. Nasrallah, A.; Lazib, Y.; Boquet, V.; Darses, B.; Dauban, P. Catalytic Intermolecular C($sp^3$)-H Amination with Sulfamates for the Asymmetric Synthesis of Amines. *Org. Process Res. Dev.* **2020**, *24*, 724–728.
11. Zalatan, D. N.; Du Bois, J. A chiral rhodium carboxamidate catalyst for enantioselective C-H amination. *J. Am. Chem. Soc.* **2008,** *130*, 9220-9221.
12. Milczek, E.; Boudet, N.; Blakey, S. Enantioselective C-H Amination Using Cationic Ruthenium(II)-Pybox Catalysts. *Angew. Chem., Int. Ed*. **2008**, *47*, 6825-6828.
13. Lang, K.; Torker, S.; Wojtas, L.; Zhang, X. P. Asymmetric Induction and Enantiodivergence in Catalytic Radical C-H Amination via Enantiodifferentiative H-Atom Abstraction and Stereoretentive Radical Substitution. *J. Am. Chem. Soc.* **2019**, *141*, 12388-12396.
14. Reddy, R. P. & Davies, H. M. Dirhodium tetracarboxylates derived from adamantylglycine as chiral catalysts for enantioselective C-H aminations. *Org. Lett.* **2006**, *8*, 5013-5016.
15. Zhou, Z.; Tan, Y.; Shen, X.; Ivlev, S.; Meggers, E. Catalytic Enantioselective Synthesis of β-Amino Alcohols by Nitrene Insertion. *Sci. China Chem.* **2021**, *64*, 452–458.
16. Modi, N. B.; Dresser, M. J.; Simon, M.; Lin, D.; Desai, D.; Gupta, S. Single- and Multiple-Dose Pharmacokinetics of Dapoxetine Hydrochloride, a Novel Agent for the Treatment of Premature Ejaculation *J. Clin. Pharmacol.* **2006**, *46*, 301-309.
17. Lang, L.; Lam, T.; Chen, A.; Jensen, C.; Duncan, L.; Kong, F. C.; Kurago, Z. B.; Shay, C.;Ten, Y. Circumventing AKT-Associated Radioresistance in Oral Cancer by Novel Nanoparticle-Encapsulated Capivasertib. *Cells* **2020**, *9*, 533.
18. Yan, L. et al. Discovery of N-[(4R)-6-(4-Chlorophenyl)-7-(2,4-dichlorophenyl)-2,2-dimethyl-3,4-dihydro-2H-pyrano[2,3-b]pyridin-4-yl]-5-methyl-1H-pyrazole-3-carboxamide (MK-5596) as a Novel Cannabinoid-1 Receptor (CB1R) Inverse Agonist for the Treatment of Obesity. *J. Med. Chem.* **2010**, *53*, 4028–4037.
19. Ju, M.; Zerull, E. E.; Roberts, J. M.; Huang, M.; Guzei, I. A.; Schomaker, J. M. Silver-Catalyzed Enantioselective Propargylic C–H Bond Amination through Rational Ligand Design *J. Am. Chem. Soc.* **2020**, *142*, 12930–12936.
20. Watkins, A. L.; Hashiguchi, B. G.; Landis, C. R. Highly enantioselective hydroformylation of aryl alkenes with diazaphospholane ligands. *Org. Lett.* **2008**, *10*, 4553-4556.
21. Liu, M.-Q.; Jiang, T. ; Chen, W.-W.; Xu, M.-H. Highly enantioselective Rh/chiral sulfur-olefin-catalyzed arylation of alkyl-substituted non-benzofused cyclic *N*-sulfonyl ketimines. *Org. Chem. Front.* **2017**, *4*, 2159-2162.
22. DFT calculations were performed at the ωB97X-D/def2-TZVPP/CPCM(DCM)//ωB97X-D/def2-TZVPP(Ag)–def2-SVP level of theory. See the SI for computational details.
23. (a) Ma, Q.; Werner, H.-J. Accurate Intermolecular Interaction Energies Using Explicitly Correlated Local Coupled Cluster Methods [PNO-LCCSD(T)-F12]. *J. Chem. Theory Comput.* **2019**, *15*, 1044–1052. (b) Ma, Q.; Werner, H. J. Scalable Electron Correlation Methods. 8. Explicitly Correlated Open-Shell Coupled-Cluster with Pair Natural Orbitals PNO-RCCSD(T)-F12 and PNO-UCCSD(T)-F12. *J. Chem. Theory Comput.* **2021**, *17*, 902–926.
24. For previous computational studies of the mechanisms of Ag nitrene C–H insertion, see: (a) Fu, Y.; Zerull, E. E.; Schomaker, J. M.; Liu, P. Origins of catalyst-controlled selectivity in the Ag-catalyzed regiodivergent C-H amination. *J. Am. Chem. Soc.* **2022**, *144*, 2735-2746. (b) Dolan, N. S.; Scamp, R. J.; Yang, T.; Berry, J. F.; Schomaker, J. M. Catalyst-controlled and tunable, chemoselective silver-catalyzed intermolecular nitrene transfer: experimental and computational studies. *J. Am. Chem. Soc.* **2016**, *138*, 14658–14667. (c) Huang, M.; Yang, T.; Paretsky, J. D.; Berry, J. F.; Schomaker, J. M. Inverting steric effects: using ″attractive″ noncovalent interactions to direct silver-catalyzed nitrene transfer. *J. Am. Chem. Soc.* **2017**, *139*, 17376–17386. (d) Weatherly, C.; Alderson, J. M.; Berry, J. F.; Hein, J. E.; Schomaker, J. M. Catalyst-controlled nitrene transfer by tuning metal:ligand ratios: insight into the mechanisms of chemoselectivity. *Organometallics* **2017**, *36*, 1649–1661.
25. Motloch, P.; Jašík, J.; Roithová, J. Gold(I) and silver(I) π-complexes with unsaturated hydrocarbons. *Organometallics* **2021**, *40*, 1492-1502.


!